

## The Dynamic Structure of Filamentous Tau\*\*

Stefan Bibow, Marco D. Mukrasch, Subashchandrabose Chinnathambi, Jacek Biernat, Christian Griesinger, Eckhard Mandelkow, and Markus Zweckstetter\*

Filaments of the protein tau are a characteristic occurrence in Alzheimer disease and many other neurodegenerative disorders<sup>[1–3]</sup> and the distribution of tau filaments correlates well with the loss of neurons and cognitive functions in Alzheimer disease.<sup>[4]</sup> Filament formation of tau filaments is based on structural transitions from random coil to  $\beta$ -structure, to give the paired helical filaments (PHFs) which share common characteristics of amyloid fibrils.<sup>[5–6]</sup>

Protease digestion and solvent-accessibility studies demonstrated that the “core” of PHFs is mainly built from repeat sequences in the C-terminal half of the tau protein.<sup>[7]</sup> The PHF core is surrounded by a “fuzzy coat”, of more than 200 residues that come from the N-terminal half of the protein as well as the C-terminus (Figure 1a).<sup>[7,8]</sup> Electron paramagnetic resonance and nuclear magnetic resonance (NMR) suggested that residues within the fuzzy coat are highly flexible.<sup>[9,10]</sup> Biochemical studies have shown that the fuzzy coat is important for tau aggregation as well as neurotoxicity.<sup>[11–13]</sup> Herein we characterized the dynamic structure of PHFs formed by 441-residue tau (htau40), the longest isoform of tau present in the human central nervous system (Figure 1a), at single-residue level using NMR spectroscopy.

We aggregated <sup>15</sup>N-labeled htau40 into insoluble filaments. NMR diffusion experiments<sup>[14]</sup> demonstrated that the observed NMR signals arises from aggregated tau protein with a molecular mass of more than 1 MDa (Figure 1b). In a two-dimensional heteronuclear single quantum coherence (HSQC) spectrum employing high-resolution magic-angle spinning (HR-MAS) (see Figure S1 in the Supporting Infor-

mation),<sup>[15]</sup> we observed about 260 signals (Figure 1c and Figure S2 and S3 in the Supporting Information). Sequence-specific resonance assignment of 244 of these signals (BMRB accession number: 17920; see Figure S2 in the Supporting Information) identified most of the residues in the N-terminal domain up to Thr212 and at the C-terminus starting at Val399.<sup>[6,10]</sup> No signals were detected for residues between Thr212 and Val399, suggesting that residues in the central domain are too immobile to be detected by liquid-state NMR spectroscopy in agreement with previous studies.<sup>[10]</sup> Comparison with monomeric htau40 revealed that the NMR resonances of many residues were strongly reduced in filamentous htau40 (Figure 1d,e). Most strikingly, the sections His121–Lys130 and Met1–Gly37 that are separated from the fibril core by 170 residues or more, showed changes in position and intensity of NMR signals (Figure 1e and Figure S2c in the Supporting Information). The presence of chemical exchange in these regions was further supported by <sup>15</sup>N spin relaxation measurements (Figure 1f and Supporting Figure S3). In agreement with chemical exchange, additional peaks were observed in close proximity to several of these residues (Figure 1f and Figure S4 in the Supporting Information). The additional signals could not be connected in triple-resonance experiments or using exchange spectroscopy because of low signal-to-noise and signal overlap. Therefore, we assigned the additional peaks to the residue for which the assigned cross-peak of the major peak set had the greatest similarity in chemical shifts and paramagnetic relaxation enhancement (see Figure S5 in the Supporting Information). This procedure indicates that the additional peaks arise from residues at the N- and C-terminus. No peak doubling was observed at the N- and C-terminus in monomeric tau (see Figure S4 in the Supporting Information), highlighting the specificity of the multiple conformations in PHF tau.

We revealed the identity of the PHF-specific conformations through measurements of paramagnetic relaxation enhancements (PREs),<sup>[17]</sup> in which nitroxide spin labels are attached to cysteine residues at various positions in the PHF tau. The resulting broadening of amide resonances caused by enhanced relaxations rate through the paramagnetic nitroxide label, is quantified through the intensity ratios in the paramagnetic and diamagnetic states (Figure 2). The PRE effect scales as the inverse sixth power of the distance between the unpaired electron of the nitroxide unit and the NMR spin, providing a powerful probe of distances. <sup>15</sup>N spin relaxation times (Figure 1f) indicate that the fuzzy coat of PHFs is highly dynamic on a broad scale suggesting that the correlation time of the electron–amide proton internuclear vector is comparable to that of small water soluble proteins. Initially, we measured PRE broadening for PHFs with a

[\*] S. Bibow, Dr. M. D. Mukrasch, Prof. Dr. C. Griesinger, Prof. Dr. M. Zweckstetter  
Department of NMR-based Structural Biology, Max Planck Institute for Biophysical Chemistry  
Am Fassberg 11, 37077 Göttingen (Germany)  
E-mail: mzwecks@gwdg.de  
S. Chinnathambi, Dr. J. Biernat, Prof. Dr. E. Mandelkow  
Max Planck Unit for Structural Molecular Biology  
c/o DESY, Notkestrasse 85, 22607 Hamburg (Germany)  
and  
DZNE, German Center for Neurodegenerative Diseases, and CAESAR, Ludwig-Erhard-Allee 2, 53175 Bonn (Germany)

[\*\*] We thank Ilka Lindner for excellent technical support and the Johann-Wolfgang-Goethe University in Frankfurt (H. Schwalbe) for lending a 900 MHz HR-MAS probehead for some measurements. This work was supported by the Max Planck Society (to E.M. and C.G.) and through the DFG (Heisenberg Scholarship to M.Z. ZW 71/2-2, 3-2 and 7-1).

Supporting information for this article is available on the WWW under <http://dx.doi.org/10.1002/anie.201105493>.

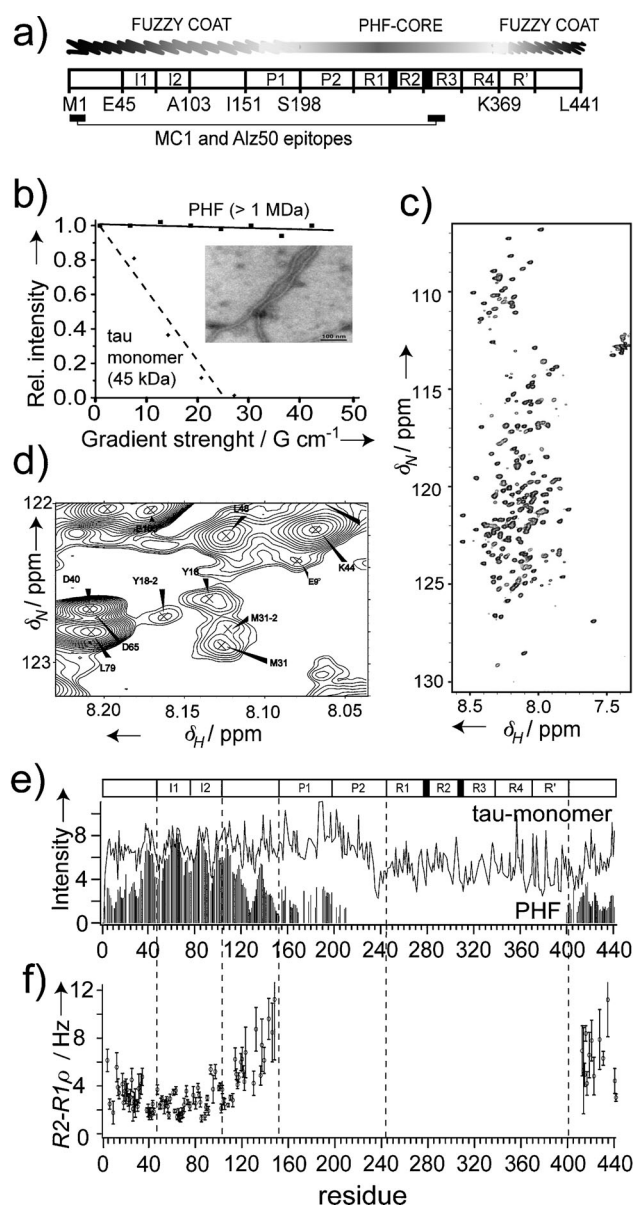


**Figure 1.** NMR spectroscopy of the dynamics in filamentous tau. a) Schematic representation of 441-residue tau with the inserts I1 and I2 that are removed by alternative splicing, the proline-rich regions P1 and P2, and the pseudo-repeats R1–R4. Top: Proposed regions for the fuzzy coat and the fibrillar core. Below: Location of the epitopes (residues 1–18 and 313–322) of the monoclonal antibodies Alz50 and MC1. b) NMR diffusion experiments for monomeric tau (dashed line) and PHF tau (solid line) with an electron micrograph from PHFs used in this study. c) 2D  $^1\text{H}$ ,  $^{15}\text{N}$ -HSQC spectrum of PHF tau. d) Selected region of the HSQC of PHF tau demonstrating the presence of multiple conformations for Tyr18 and Met31. e) Comparison of absolute signal intensities of PHF tau (bars) and monomeric tau (line). f) Relaxation rates illustrating significant motions in the  $\mu\text{s}$ – $\text{ms}$  time-scale for the N-terminus of filamentous tau.

nitroxide attached to position 15 (Figure 2 a–c); 40 residues at the N-terminus were broadened with PRE intensity ratios below 0.6. In addition, NMR spectroscopy revealed that Ala119–Asp133, the proline-rich region (Ile151–Thr212) and the C-terminal fuzzy coat (Val399–Ala429) are in transient contact with the N-terminus of PHF tau. The similarity of the

PRE intensity ratio profile (Figure 2b) with the pattern of NMR signal intensities of PHF tau (Figure 1e) suggests that the PHF-specific conformations are caused by formation of transient long-range interactions. The global folding of the fuzzy coat of PHFs was further supported by paramagnetic effects observed for a nitroxide radical at position 125 (Figure 2 d, e, f). Control experiments prove that the observed paramagnetic effects are mostly of intramolecular nature (see Figure S6 in the Supporting Information).

To directly probe the interaction between the fibril core and the fuzzy coat, we attached the nitroxide spin label to the native cysteine Cys322 of filamentous tau (Figure 2g–i). Attachment of the nitroxide label to Cys322 caused signal broadening in residue stretches close to Gln124, a region that transiently populates helical conformations (see Figure S7 in the Supporting Information), Ala152 and Asn167–Thr212, as well as Ser409–Ala426 at the C-terminus. Thus, residues in the projection domain and at the C-terminus contact the PHF-core residue Cys322 consistent with partial protection of the C-terminus to proteolysis in PHF tau.<sup>[18]</sup> The strongest effect, however, was observed for the first 30 residues at the N-terminus using either the major or the minor peak set observed for the N-terminal residues (Figure 2h and Figure S5c in the Supporting Information). Taken together NMR spectroscopy revealed a network of long-range interactions between conserved regions of filamentous tau.

To obtain insight into the mechanism of formation of long-range interactions in PHF tau, we performed NMR measurements of PHF tau at high ionic strength and of a mutant version of PHF tau in which Phe8 and Val10 were replaced by serine. Mutation of Phe8 and Val10, two hydrophobic residues at the N-terminus of tau, did not affect chemical exchange broadening in PHF tau (Figure 3a). In contrast, at high ionic strength the intensity profile of PHF tau was very similar to the profile observed for monomeric tau (Figure 3b). Only in regions neighboring the fibril core, that is residues 170–212 and 399–441, the intensity in the fuzzy coat remained low, most likely due to restricted motion inferred by the nearby fibril core. The strong impact of ionic strength demonstrates that electrostatic interactions are important for formation of the network of intramolecular long-range interactions in PHF tau.

For improved Alzheimer disease diagnosis antibodies were developed that detect changes in the conformation of tau.<sup>[19–21]</sup> The monoclonal antibodies Alz50 and MC1 recognize conformational changes in the tau protein that appear before the assembly of PHFs and are then also found in PHF, but are not present in normal brain.<sup>[20,22]</sup> The specificity of Alz50 and MC1 for pathological tau is due to a unique conformation of tau in the disease state and requires two discontinuous epitopes that are separated by about 300 residues and are located at the N-terminus (residues 1–18) and in the repeat region (residues 313–322).<sup>[20,22,23]</sup> Our paramagnetic NMR measurements demonstrated that the two discontinuous epitopes are in transient contact and are part of a network of long-range interactions that links the fuzzy coat with the PHF core (Figure 2). Comparison with NMR measurements in monomeric tau (Figure 3c and Figure S8 in the Supporting Information) showed that the paramagnetic

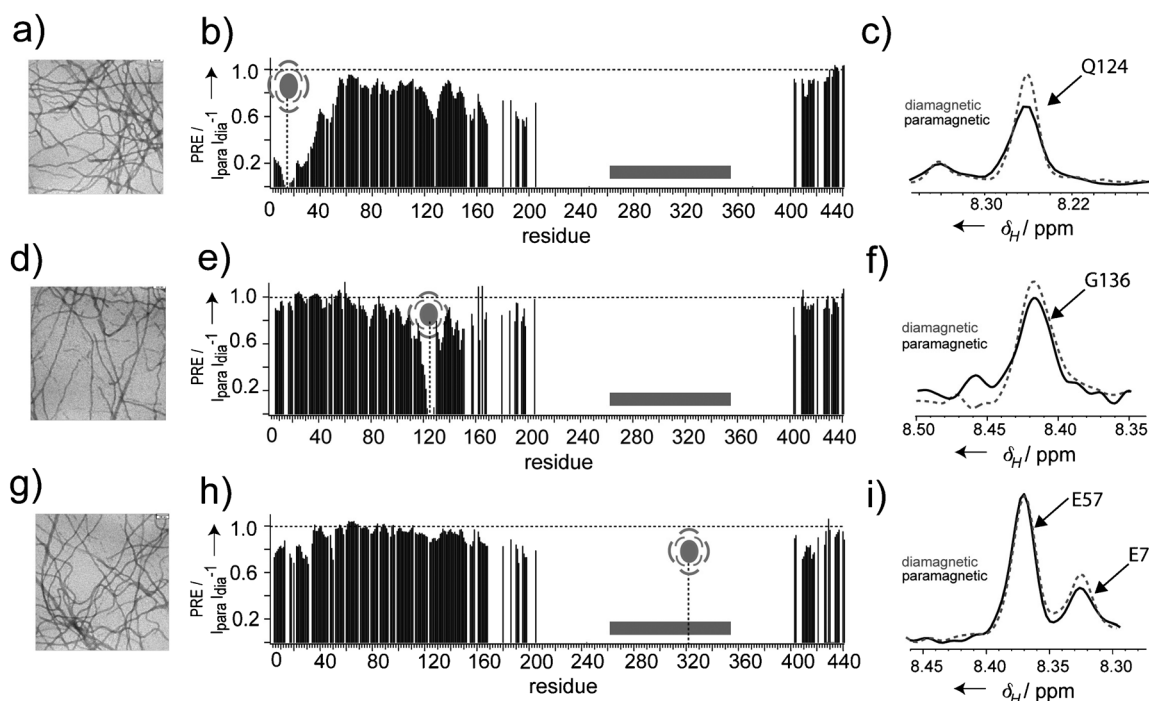


**Figure 2.** Transient long-range contacts in filamentous tau. a)–c) Paramagnetic NMR of PHFs with the nitroxide label attached at position 15. a) Electron micrograph, b) PRE profiles of amide protons, and c) selected region from  $[^1\text{H}, ^{15}\text{N}]$ -HSQC in the paramagnetic (black) and diamagnetic state (gray dashed line). Intensity ratios were averaged over a three-residue window. Decreases in peak intensity ratios that occur far from the site of spin-labeling (more than 10 residues) are indicative of long-range contacts ( $< 25 \text{ \AA}$ ) between the spin-label and distant areas of sequence. The location of the fibril core identified by solid-state NMR spectroscopy is shown as a gray bar. d)–f) Paramagnetic NMR of PHFs with the nitroxide label attached at position 125. g)–i) Paramagnetic NMR of PHFs with the nitroxide label attached at the native Cys322.

effects induced at the N-terminus became stronger in PHF tau demonstrating that the interaction between the two discontinuous epitopes of the monoclonal Alz50 and MC1 antibodies is tightened in PHF tau. In addition, PHF-specific long-range contacts were observed between the proline-rich domain, the region next to Met127 and the N- and C-terminus. The network of long-range contacts involving several regions in filamentous tau explains the requirement of residues 155–244 and 305–314 for recognition by the conformation-specific antibody Tau66,<sup>[24]</sup> as well as the attenuation of Alz50 and MC1 antibody reactivity upon deletion of residues 46–241.<sup>[25]</sup> In addition, the observed long-range contacts are mostly intramolecular despite the high local concentration of tau in PHFs, in agreement with failed attempts at creating the Alz50 and MC1 epitopes intermolecularly by combining complementary  $\text{NH}_2$ - and  $\text{COOH}$ -terminal deletion mutants with an epitope.<sup>[20,22]</sup>

There is increasing evidence that soluble oligomeric tau species, rather than filamentous tau, may be the critical toxic moiety underlying neurodegeneration.<sup>[26]</sup> Biochemical studies using recombinant tau have demonstrated a clear selectivity of Alz50 and MC1 for PHF tau: the interaction of Alz50 with PHF-tau is nearly two orders of magnitude greater in affinity than its interaction with recombinant monomeric tau.<sup>[25]</sup> However, MC1 and Alz50 also bind to a non-filamentous, soluble pool of abnormal tau that is able to self-assemble into PHFs in a concentration-dependent manner,<sup>[27]</sup> suggesting that both PHFs and soluble oligomers of tau are recognized

by Alz50 and MC1. Our study reveals that the two epitopes of the Alz50 and MC1 antibody are already weakly in contact in monomeric tau, but the interaction is tightened during aggregation (Figure 3c) providing a potential mechanism for the recognition of both oligomeric and PHF tau.

In summary, our study demonstrates that the core structure of tau filaments interacts with otherwise unstructured segments within the protein (Figure 4). It rationalizes the conformation-specific antibodies of tau and highlights the heterogeneity within aggregate structures.

### Experimental Section

**Recombinant preparation of tau:** Expression, purification, and isotope labeling of wild-type and mutant htau40 were performed as described previously.<sup>[28]</sup> NMR samples contained  $^{15}\text{N}$ - or  $^{13}\text{C}/^{15}\text{N}$ -labeled protein in 95%  $\text{H}_2\text{O}/5\% \text{D}_2\text{O}$  and 50 mM phosphate buffer, pH 6.8.

**Spin labeling of tau:** Spin labeling of tau was performed as described previously.<sup>[28]</sup> To probe for intermolecular contacts, a 1:1 mixture of  $^{14}\text{N}$  C15A291/G322-htau40 and  $^{15}\text{N}$ -labeled A291/G322-htau40 was prepared. The nitroxide spin label MTSL was attached to  $^{14}\text{N}$ -labeled C15A291/G322-htau40 prior to mixing and aggregation.

**Formation of paired helical filaments:** PHFs of wild-type and mutant htau40 were formed by mixing  $^{13}\text{C}/^{15}\text{N}$  or  $^{15}\text{N}$ -labeled protein (ca. 1.5 mM) with heparin 5000 (heparin:tau 1:4) and incubation at 37°C for 4 days. The reaction was then pelleted at 160000 g for 40 min. The protein supernatant was complemented again with heparin and incubated for another 4 days. To remove any residual monomeric tau as well as the aggregation inducer heparin, PHF

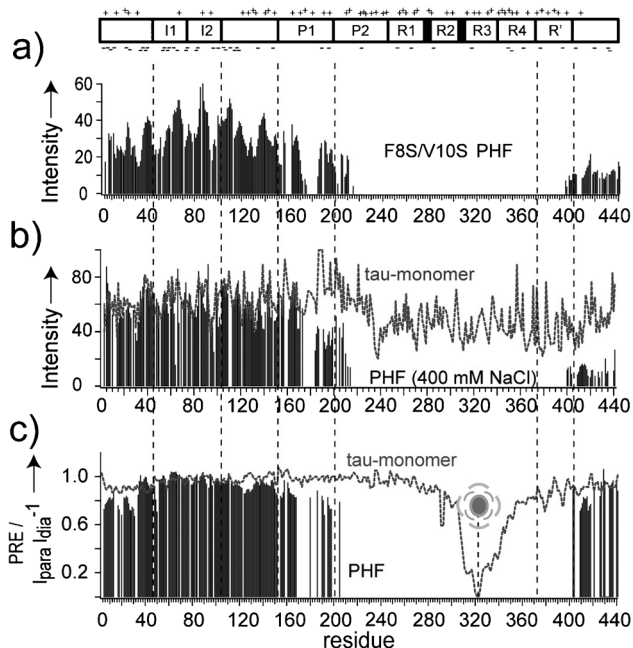


**Figure 3.** Ionic-strength dependence of transient interactions in filamentous tau. a) NMR signal intensities observed in a 2D [ $^1\text{H}$ ,  $^{15}\text{N}$ ]-HSQC of mutant PHF tau, in which Phe8 and Val10 were replaced by serine. b) Comparison of absolute NMR signal intensities in PHF tau at increased ionic strength (400 mM NaCl; bars) and in monomeric tau (gray dashed line). c) Comparison of the PRE intensity profile of monomeric tau (gray dashed line) and PHF tau (bars), when a nitroxide spin label was attached to the native Cys322. At the N-terminus, PRE intensity ratios are lower in PHF tau than in monomeric tau revealing a tightening of long-range contacts. Top: The domain organization of htau40 and the location of negative and positive charges.

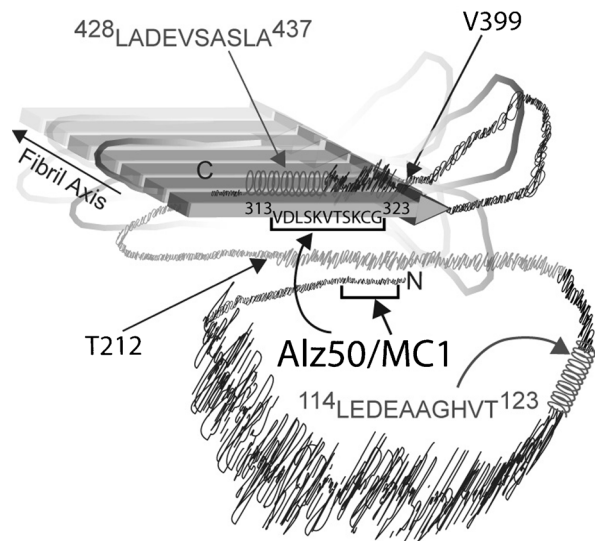


**Figure 4.** Model of the network of long-range interactions specific for PHF tau. Regions of transient helical structure are indicated. The gray bars with arrow heads represent the fibrillar core identified by solid-state NMR spectroscopy. Higher NMR signal intensities in the fuzzy coat are indicated by an increasing width of the protein chain. Spatial proximity between different parts of the chain indicates tertiary contacts that were revealed by paramagnetic NMR experiments. The two discontinuous epitopes of the conformation-specific antibodies Alz50 and MC1, residues 1–18 and 313–322, are labeled.

pellets were ultracentrifuged, the pellets were washed with fresh buffer not containing heparin and centrifuged again (40000 rpm, 4°C, 40 min). The steps were repeated at least 3 times prior to the NMR measurements. 1D NMR spectra demonstrated that no residual heparin was left (see Figure S1 in the Supporting Information).

**NMR spectroscopy:** NMR experiments were conducted on a 900 MHz spectrometer (Bruker) at 278 K. NMR samples contained 40–80 mg of htau40 fibrils in a volume of 60  $\mu\text{L}$ . A 3D constant-time HNCA experiment was recorded with a HR-MAS spinning frequency of 6 kHz,  $2048 \times 68 \times 88$  points ( $^1\text{H} \times ^{13}\text{C} \times ^{15}\text{N}$ ) and 50 scans, resulting in a total experimental time of 4 days and 3 h. PRE effects were measured from the peak intensity ratios between two 2D  $^{15}\text{N}$ - $^1\text{H}$  HSQC NMR spectra of PHF tau, which was tagged with a nitroxide spin label, before and after addition of 4 mM DTT (dithio threitol) heated to 42°C for 30 min before measurement.

Full Methods are available in the Supporting Information.

Received: August 3, 2011

Published online: October 11, 2011

**Keywords:** aggregation · Alzheimer disease · fuzzy coat · paired helical filament · tau protein

- [1] C. Ballatore, V. M. Lee, J. Q. Trojanowski, *Nat. Rev. Neurosci.* **2007**, *8*, 663–672.
- [2] C. Haass, D. J. Selkoe, *Nat. Rev. Mol. Cell Biol.* **2007**, *8*, 101–112.
- [3] S. A. Small, K. Duff, *Neuron* **2008**, *60*, 534–542.
- [4] H. Braak, E. Braak, *Acta Neuropathol.* **1991**, *82*, 239–259.
- [5] J. Berriman, L. C. Serpell, K. A. Oberg, A. L. Fink, M. Goedert, R. A. Crowther, *Proc. Natl. Acad. Sci. USA* **2003**, *100*, 9034–9038.
- [6] O. C. Andronesi, M. von Bergen, J. Biernat, K. Seidel, C. Griesinger, E. Mandelkow, M. Baldus, *J. Am. Chem. Soc.* **2008**, *130*, 5922–5928.
- [7] C. M. Wischik, M. Novak, P. C. Edwards, A. Klug, W. Tichelaar, R. A. Crowther, *Proc. Natl. Acad. Sci. USA* **1988**, *85*, 4884–4888.
- [8] T. A. Schoenfeld, R. A. Obar, *Int. Rev. Cytol.* **1994**, *151*, 67–137.
- [9] M. Margittai, R. Langen, *Proc. Natl. Acad. Sci. USA* **2004**, *101*, 10278–10283.
- [10] A. Sillen, J. M. Wieruszeski, A. Leroy, A. B. Younes, I. Landrieu, G. Lippens, *J. Am. Chem. Soc.* **2005**, *127*, 10138–10139.
- [11] Y. Wang, S. Garg, E. M. Mandelkow, E. Mandelkow, *Biochem. Soc. Trans.* **2010**, *38*, 955–961.
- [12] N. E. LaPointe, G. Morfini, G. Pigino, I. N. Gaisina, A. P. Kozikowski, L. I. Binder, S. T. Brady, *J. Neurosci. Res.* **2009**, *87*, 440–451.
- [13] P. M. Horowitz, N. LaPointe, A. L. Guillozet-Bongaarts, R. W. Berry, L. I. Binder, *Biochemistry* **2006**, *45*, 12859–12866.
- [14] E. O. Stejskal, J. E. Tanner, *J. Chem. Phys.* **1965**, *42*, 288–292.
- [15] A. N. Garroway, *J. Magn. Reson.* **1982**, *49*, 168–171.
- [16] A. Sillen, J.-M. Wieruszeski, A. Leroy, A. B. Younes, I. Landrieu, G. Lippens, *J. Am. Chem. Soc.* **2005**, *127*, 10138–10139.
- [17] J. R. Gillespie, D. Shortle, *J. Mol. Biol.* **1997**, *268*, 170–184.
- [18] M. von Bergen, S. Barghorn, S. A. Muller, M. Pickhardt, J. Biernat, E. M. Mandelkow, P. Davies, U. Aebi, E. Mandelkow, *Biochemistry* **2006**, *45*, 6446–6457.
- [19] E. M. Sigurdsson, *Curr. Alzheimer Res.* **2009**, *6*, 446–450.
- [20] G. A. Jicha, R. Bowser, I. G. Kazam, P. Davies, *J. Neurosci. Res.* **1997**, *48*, 128–132.
- [21] M. Mercken, M. Vandermeeren, U. Lubke, J. Six, J. Boons, A. Van de Voorde, J. J. Martin, J. Gheuens, *Acta Neuropathol.* **1992**, *84*, 265–272.
- [22] G. Carmel, E. M. Mager, L. I. Binder, J. Kuret, *J. Biol. Chem.* **1996**, *271*, 32789–32795.

- [23] G. A. Jicha, B. Berenfeld, P. Davies, *J. Neurosci. Res.* **1999**, *55*, 713–723.
- [24] N. Ghoshal, F. Garcia-Sierra, Y. Fu, L. A. Beckett, E. J. Mufson, J. Kuret, R. W. Berry, L. I. Binder, *J. Neurochem.* **2001**, *77*, 1372–1385.
- [25] G. A. Jicha, R. Bowser, I. G. Kazam, P. Davies, *J. Neurosci. Res.* **1997**, *48*, 128–132.
- [26] A. de Calignon, L. M. Fox, R. Pitstick, G. A. Carlson, B. J. Bacskai, T. L. Spires-Jones, B. T. Hyman, *Nature* **2010**, *464*, 1201–1204.
- [27] C. L. Weaver, M. Espinoza, Y. Kress, P. Davies, *Neurobiol. Aging* **2000**, *21*, 719–727.
- [28] M. D. Mukrasch, S. Bibow, J. Korukottu, S. Jeganathan, J. Biernat, C. Griesinger, E. Mandelkow, M. Zweckstetter, *PLoS Biol.* **2009**, *7*, e34.
-